INTRODUCTION & OVERVIEW OF THE URQMD MODEL FOR PP, PA AND AA

Marcus Bleicher
Institut für Theoretische Physik
Goethe Universität – Frankfurt
Germany

Ultra-relativistic Quantum Molecular Dynamics (UrQMD)

- Based on the propagation of hadrons, following relativistic Hamilton equations of motion
- Nuclear potentials (hard/soft/EoS) can be switched on
- Rescattering among hadrons is fully included, based on available cross sections
- The collision term includes the interaction of approx. 100x100 hadrons (incl. particles and anti-particles)
- String excitation/decay at higher energies (LUND picture + PYTHIA)
- Provides a solution for the time dependent n-particle phase space distribution of all hadrons
- Includes event-by-event fluctuations, correlations, clusters, ...

M. Bleicher et al, J.Phys. G25 (1999) 1859-1896

Side remark: difference to BUU models

- BUU models solve a version of the relativistic Boltzmann equation

$$p^{\mu} \cdot \partial_{\mu} f_i(x^{\nu}, p^{\nu}) = \mathcal{C}_i$$

- Provides an averaged 1-particle time dependent phase space distribution
  - No physical fluctuations (deterministic PDE, no e-by-e fluc's)
  - No correlations, no clusters (these are 2-particle correlations)
  - Energy conservation only on average
  - In full ensemble calculations: self interaction of hadrons

M. Bleicher et al, J.Phys. G25 (1999) 1859-1896

nucleon	Δ	Λ	Σ	Ξ	Ω
N_{938}	Δ_{1232}	Λ_{1116}	Σ_{1192}	Ξ_{1317}	Ω_{1672}
N_{1440}	Δ_{1600}	Λ_{1405}	Σ_{1385}	Ξ_{1530}	
N_{1520}	Δ_{1620}	Λ_{1520}	Σ_{1660}	Ξ_{1690}	
N_{1535}	Δ_{1700}	Λ_{1600}	Σ_{1670}	Ξ_{1820}	
N_{1650}	Δ_{1900}	Λ_{1670}	Σ_{1775}	Ξ_{1950}	
N_{1675}	Δ_{1905}	Λ_{1690}	Σ_{1790}	Ξ_{2025}	
N_{1680}	Δ_{1910}	Λ_{1800}	Σ_{1915}		
N_{1700}	Δ_{1920}	Λ_{1810}	Σ_{1940}		
N_{1710}	Δ_{1930}	Λ_{1820}	Σ_{2030}		
N_{1720}	Δ_{1950}	Λ_{1830}			
N_{1900}		Λ_{1890}			
N_{1990}		Λ_{2100}			
N_{2080}		Λ_{2110}			
N_{2190}					
N_{2200}					
N_{2250}					

0^{-+}	1^{--}	0^{++}	1^{++}
π	ρ	a_0	a_1
K	K^*	K_0^*	K_1^*
η	ω	f_0	f_1
η'	ϕ	f_0^*	f_1'
1^{+-}	2^{++}	$(1^{--})^*$	$(1^{--})^{**}$
b_1	a_2	ρ_{1450}	ρ_{1700}
K_1	K_2^*	K_{1410}^*	K_{1680}^*
h_1	f_2	ω_{1420}	ω_{1662}
h_1'	f_2'	ϕ_{1680}	ϕ_{1900}

List of included particles in the hadron cascade

- Binary interactions between all implemented particles are treated individually
- Cross sections are taken from data when available or models
- Resonances are implemented in Breit-Wigner form
- No a priori in-medium modifications, however collisional broadening and mass dependent decay widths are included

Baryon-baryon scattering cross section I

- The total NN cross section is given by the sum of all resonance states + strings towards higher energies

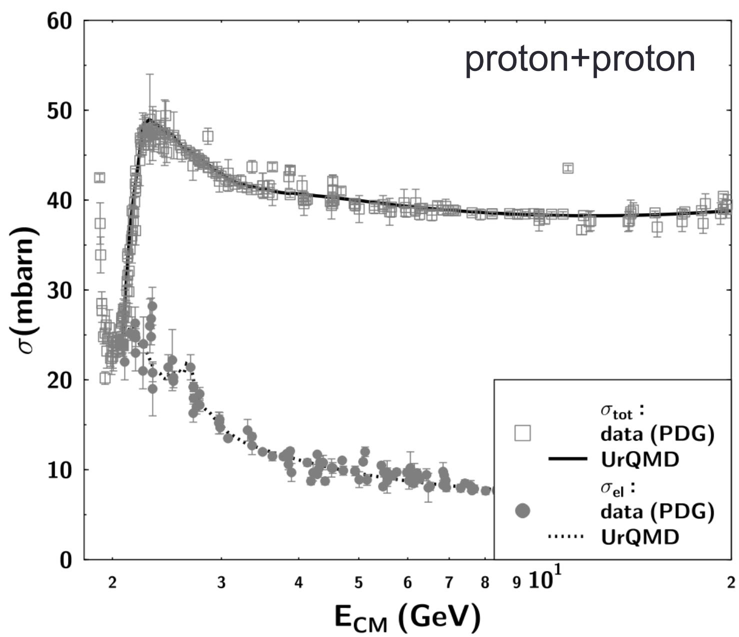

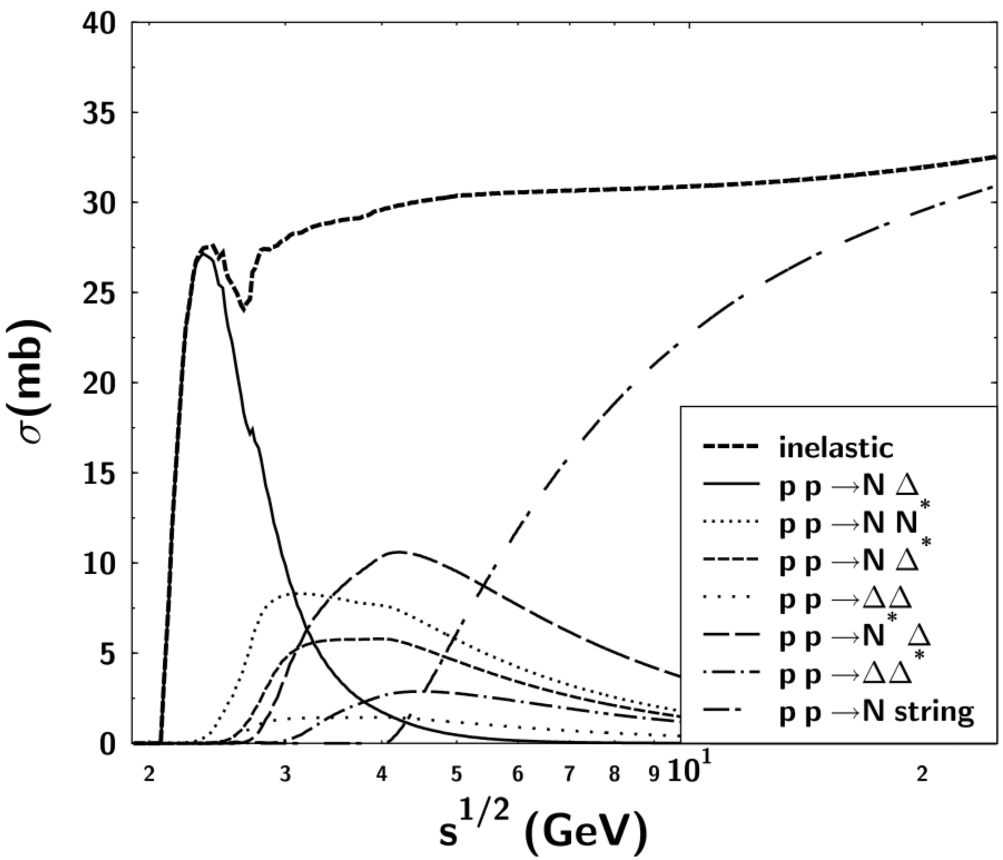

Baryon-baryon scattering cross section II

- Phase space x matrix element:

$$\sigma_{tot}^{BB}(\sqrt{s}) \propto (2S_D+1)(2S_E+1)\frac{\langle p_{D,E}\rangle}{\langle p_{A,C}\rangle}\frac{1}{s}|\mathcal{M}|^2$$

- Matrix element is fitted to data for groups of resonance channels
- Detailed balance is fulfilled for the inverse reaction:

$$\sigma(y \to x)\, p_y^2\, g_y = \sigma(x \to y)\, p_x^2\, g_x$$

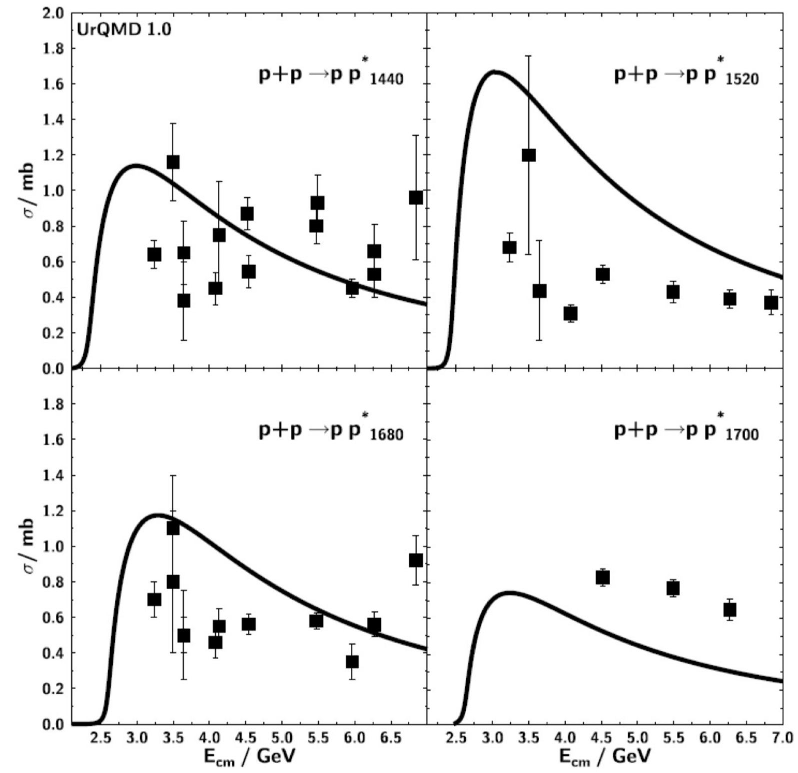

Mass dependent branching ratios

- Decay branches of resonances depend on available phase space (→ mass dependent branching ratios)

$$\Gamma_{i,j}(M) = \Gamma_R^{i,j} \frac{M_R}{M} \left(\frac{\langle p_{i,j}(M) \rangle}{\langle p_{i,j}(M_R) \rangle} \right)^{2l+1} \frac{1.2}{1 + 0.2 \left(\frac{\langle p_{i,j}(M) \rangle}{\langle p_{i,j}(M_R) \rangle} \right)^{2l}}$$

$$\Gamma_{tot}(M) = \sum_{br=\{i,j\}}^{N_{br}} \Gamma_{i,j}(M)$$

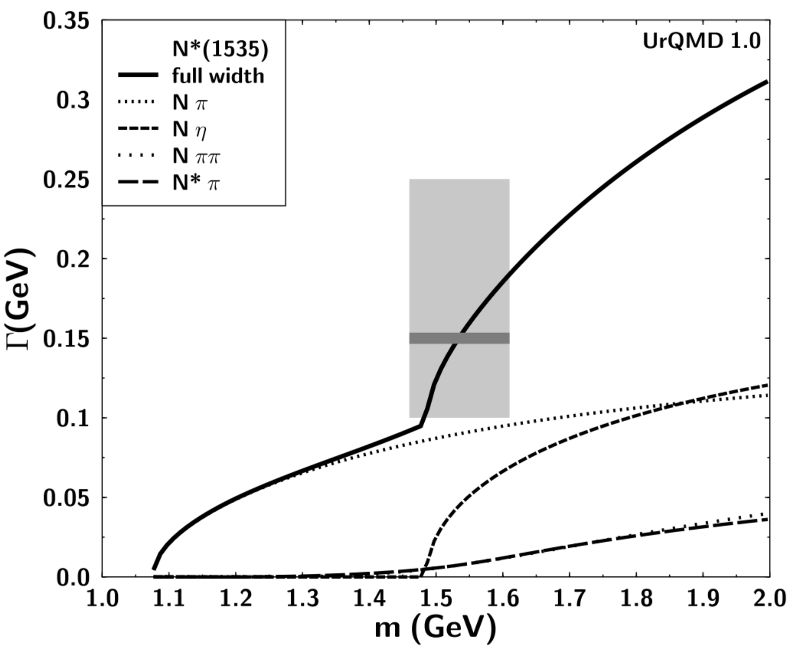

→

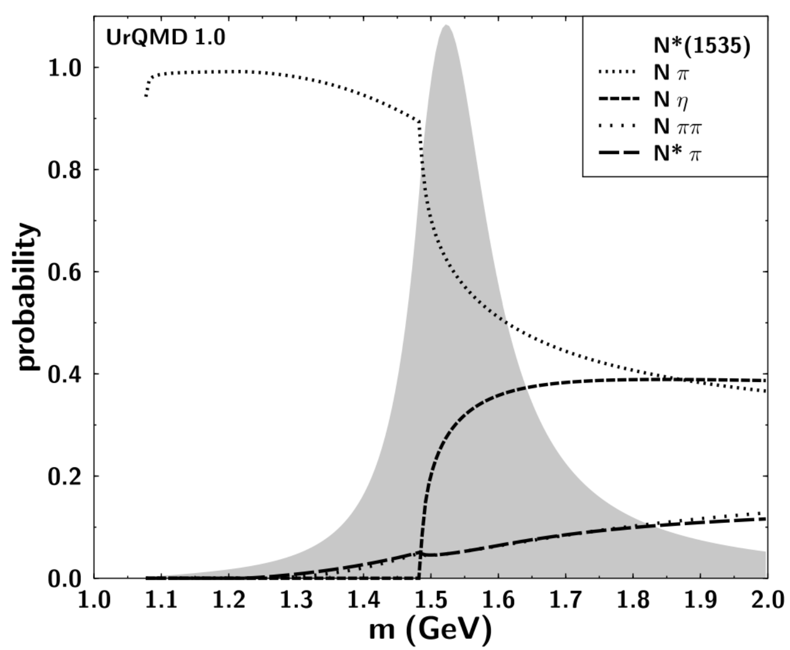

Meson production in pp I

- Exclusive and inclusive production of selected mesons

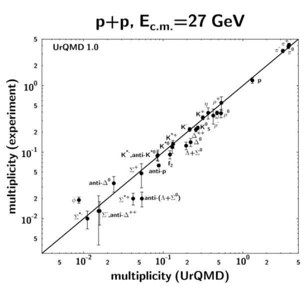

$$\epsilon = \sqrt{s} - \sqrt{s_{th}}$$

$$\sqrt{s_{th}} = 2m_p + m_m$$

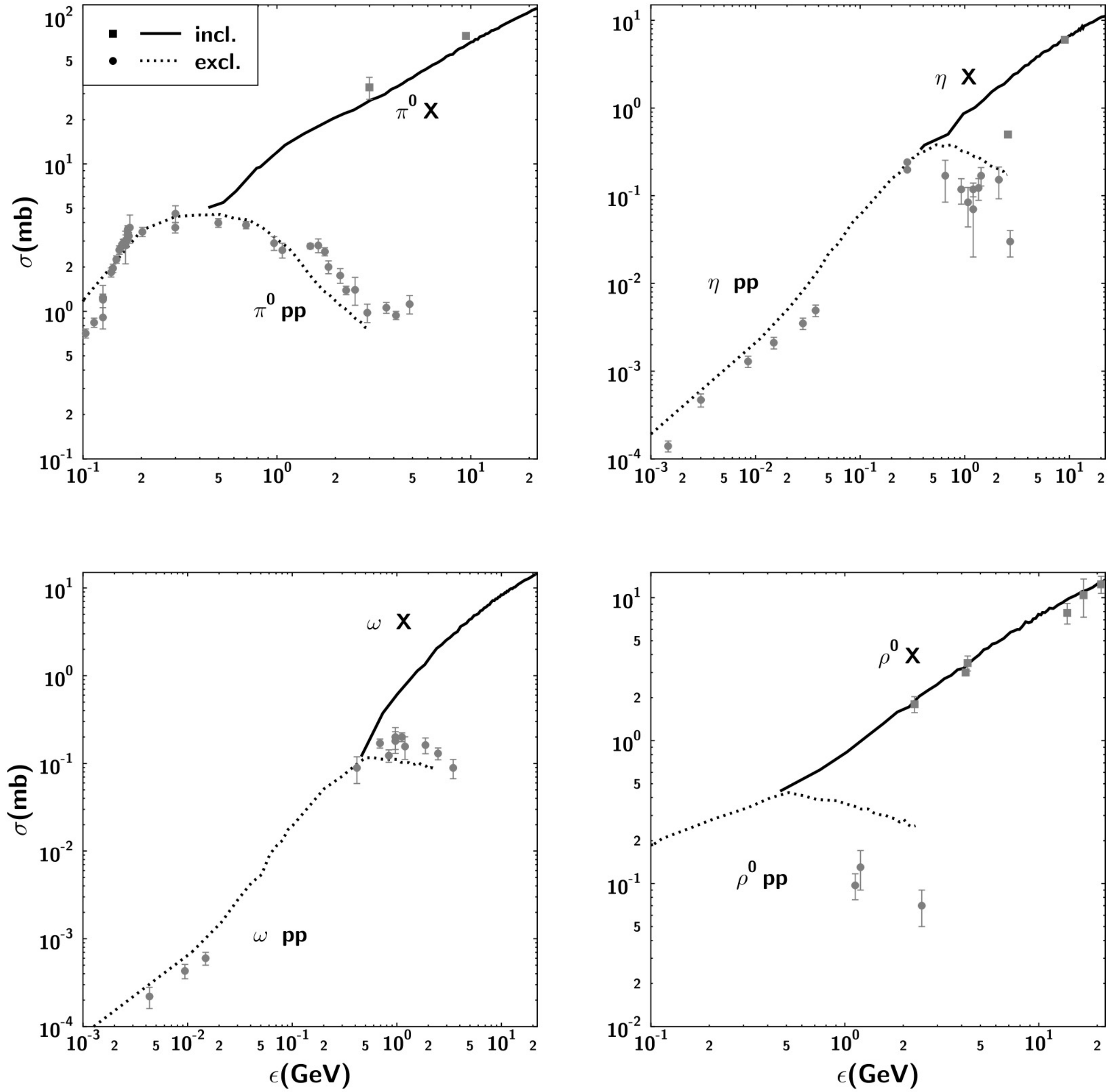

Meson production in pp II

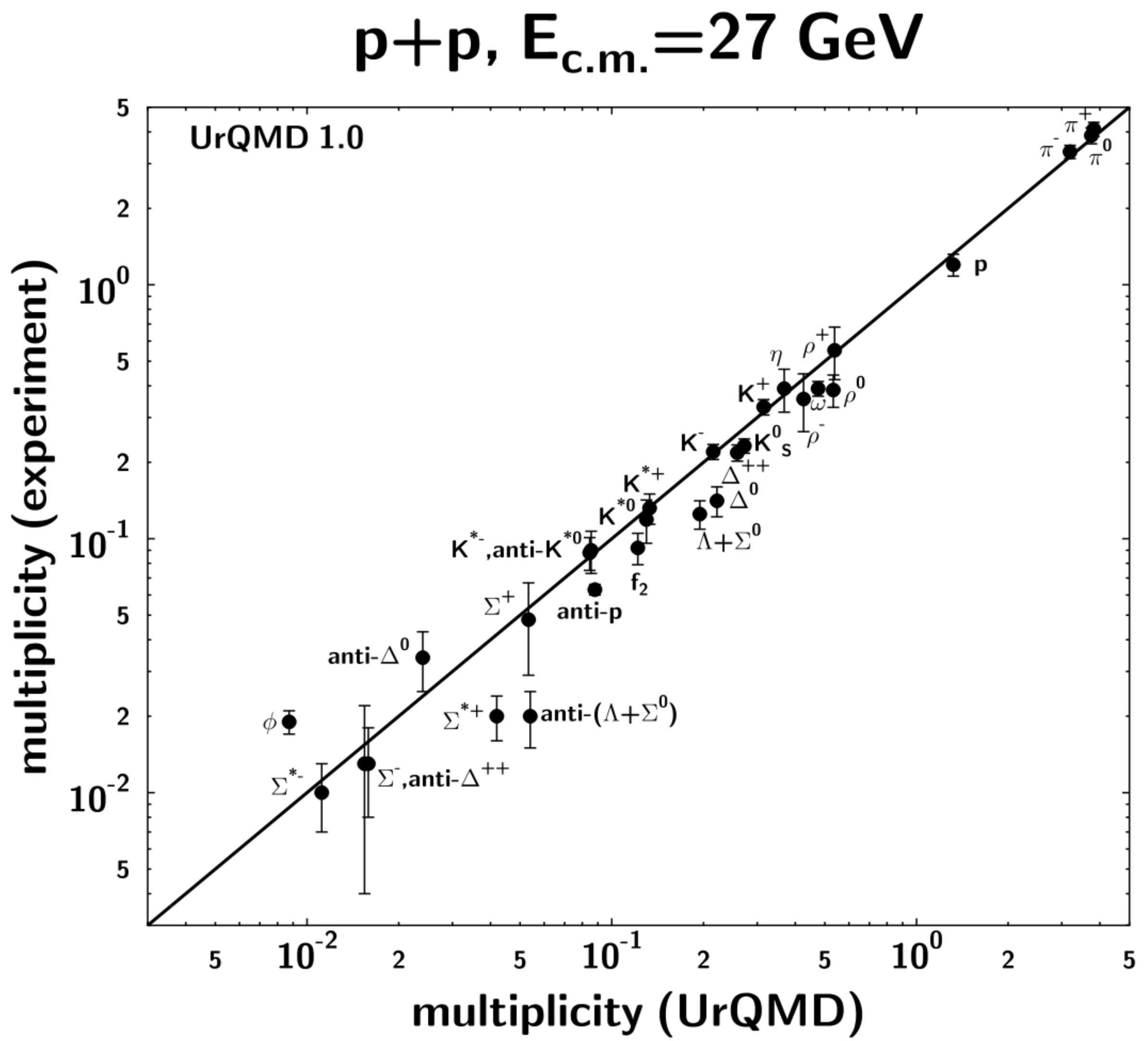

Meson-baryon scattering cross sections (→ baryonic resonances)

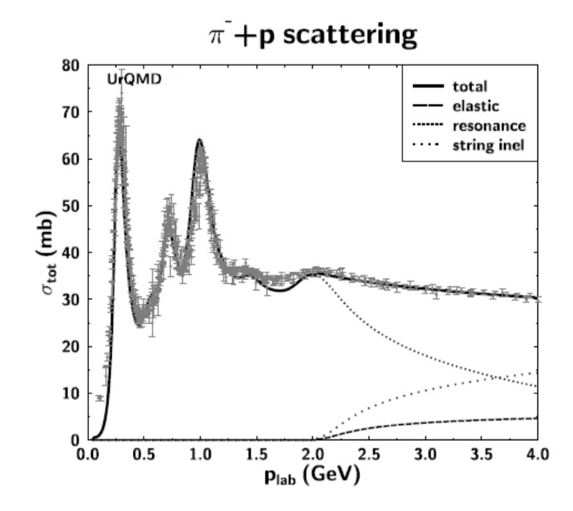

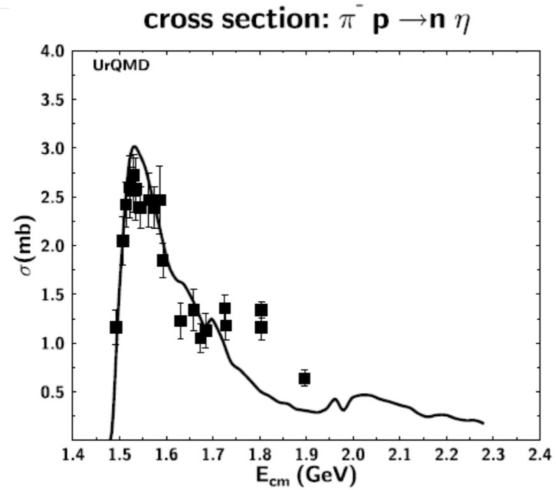

resonance	mass	width	$N\gamma$	$N\pi$	$N\eta$	$N\omega$	$N\varrho$	$N\pi\pi$	$\Delta_{1232}\pi$	$N^*_{1440}\pi$	ΛK
N^*_{1440}	1.440	200		0.70				0.05	0.25		
N^*_{1520}	1.520	125		0.60				0.15	0.25		
N^*_{1535}	1.535	150	0.001	0.55	0.35			0.05		0.05	
N^*_{1650}	1.650	150		0.65	0.05			0.05	0.10	0.05	0.10
N^*_{1675}	1.675	140		0.45					0.55		
N^*_{1680}	1.680	120		0.65				0.20	0.15		
N^*_{1700}	1.700	100		0.10	0.05		0.05	0.45	0.35		
N^*_{1710}	1.710	110		0.15	0.20		0.05	0.20	0.20	0.10	0.10
N^*_{1720}	1.720	150		0.15			0.25	0.45	0.10		0.05
N^*_{1900}	1.870	500		0.35		0.55	0.05		0.05		
N^*_{1990}	1.990	550		0.05			0.15	0.25	0.30	0.15	0.10
N^*_{2080}	2.040	250		0.60	0.05		0.25	0.05	0.05		
N^*_{2190}	2.190	550		0.35			0.30	0.15	0.15	0.05	
N^*_{2220}	2.220	550		0.35			0.25	0.20	0.20		
N^*_{2250}	2.250	470		0.30			0.25	0.20	0.20	0.05	
Δ_{1232}	1.232	115.	0.01	1.00							
Δ^*_{1600}	1.700	200		0.15					0.55	0.30	
Δ^*_{1620}	1.675	180		0.25					0.60	0.15	
Δ^*_{1700}	1.750	300		0.20			0.10		0.55	0.15	
Δ^*_{1900}	1.850	240		0.30			0.15		0.30	0.25	
Δ^*_{1905}	1.880	280		0.20			0.60		0.10	0.10	
Δ^*_{1910}	1.900	250		0.35			0.40		0.15	0.10	
Δ^*_{1920}	1.920	150		0.15			0.30		0.30	0.25	
Δ^*_{1930}	1.930	250		0.20			0.25		0.25	0.30	
Δ^*_{1950}	1.950	250	0.01	0.45			0.15		0.20	0.20	

$$\sigma^{MB}_{tot}(\sqrt{s}) = \sum_{R=\Delta,N^*} \langle j_B, m_B, j_M, m_M \| J_R, M_R \rangle \frac{2S_R+1}{(2S_B+1)(2S_M+1)} \times \frac{\pi}{p^2_{cm}} \frac{\Gamma_{R\to MB}\Gamma_{tot}}{(M_R-\sqrt{s})^2+\Gamma^2_{tot}/4} ,$$

Meson-baryon scattering (→ meson resonances)

- Meson-meson scattering in the resonance region is treated in analogy to the meson-baryon scattering
- At higher energies, also t-channel excitation is taken into account

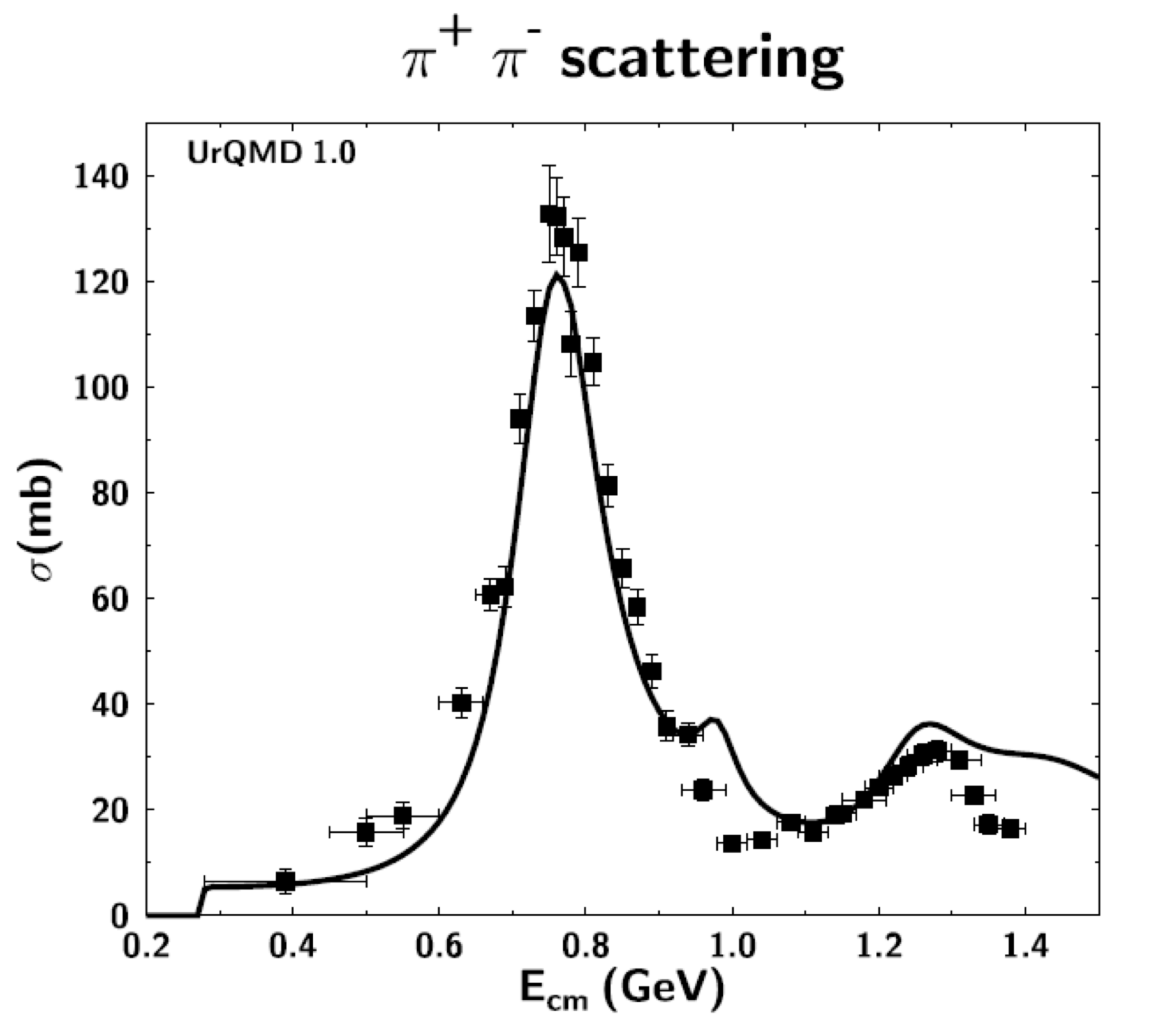

Comparison to low energy data (pion beam)

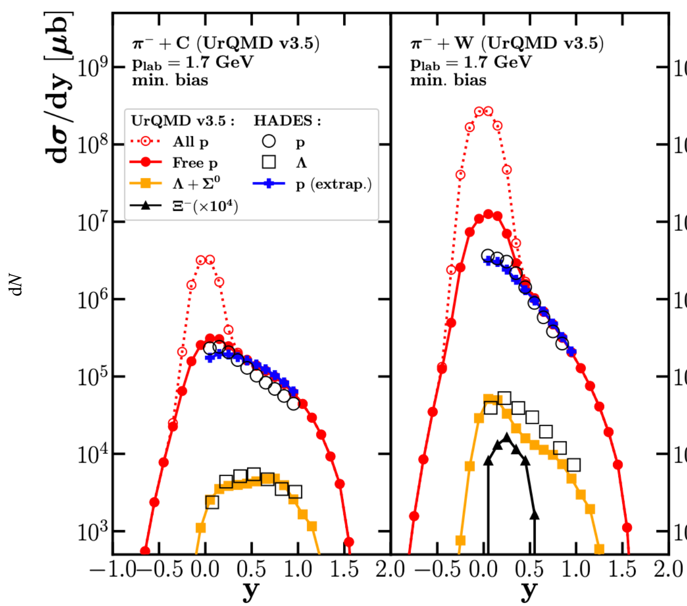

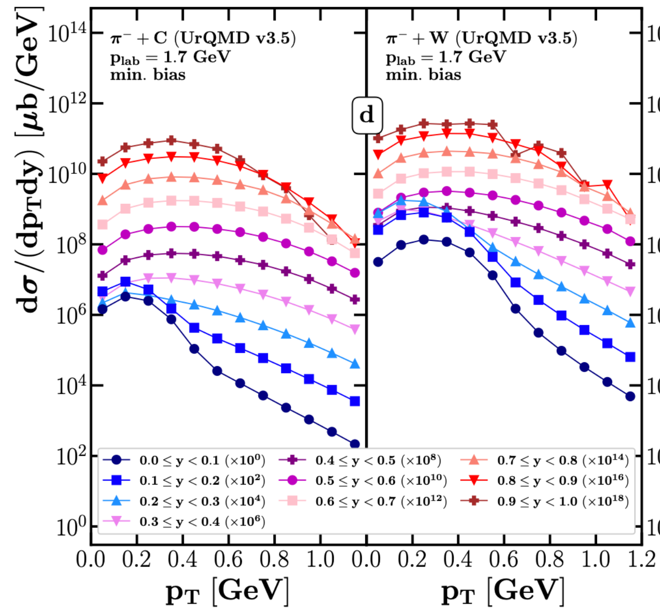

Proton and Lambda rapidity distribution in π+C, π+W reaction at p_{lab}=1.7 GeV

Deuteron production (transverse momentum spectra) in π+C, π+W reaction at p_{lab}=1.7 GeV

- Baryon knockout in line with data at low pion momenta, also substantial production of clusters

A. Kittiratpattana, M. Bleicher et al, e-Print: 2305.09208

Comparison to low energy data (small systems)

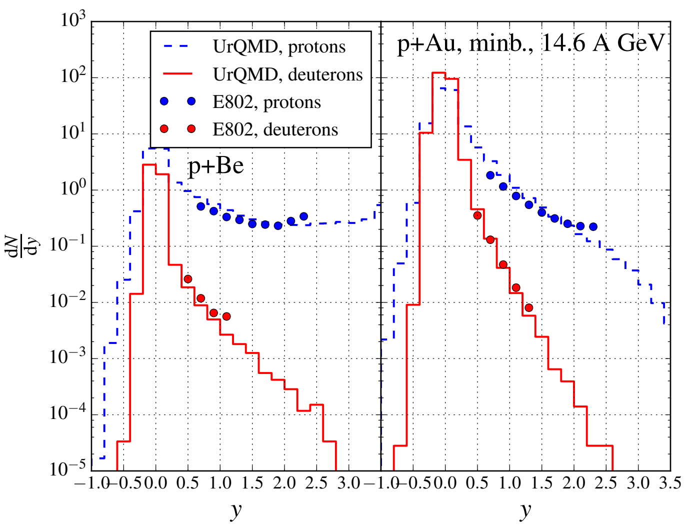

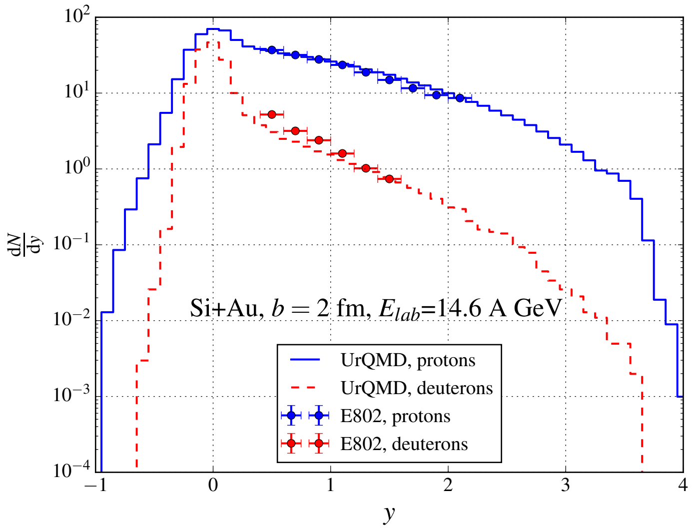

Proton and deuteron rapidity distribution in p+Be, p+Au reaction at E_{lab}=14.6 AGeV

Proton and deuteron rapidity distribution for Si+Au reactions at E_{lab}=14.6 AGeV

- Baryon energy loss in line with data at low energies

S. Sombun, M. Bleicher et al, arXiv:1805.11509

Side remark on anti-deuterons

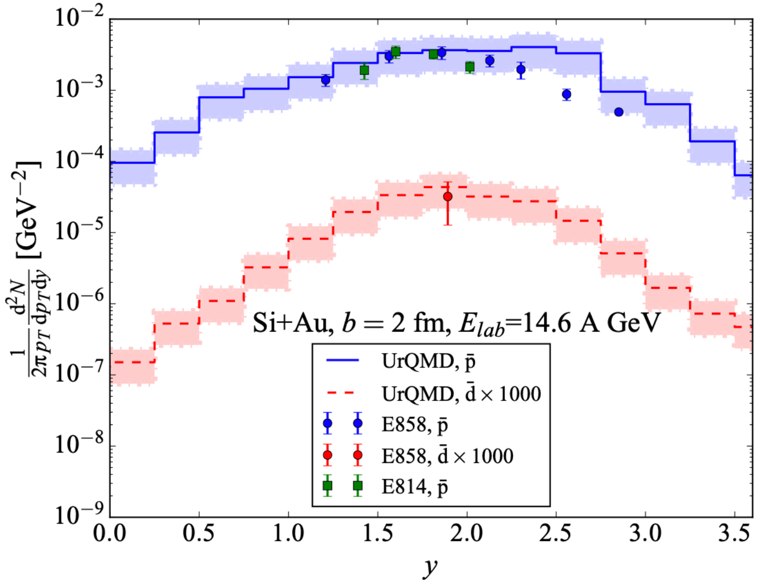

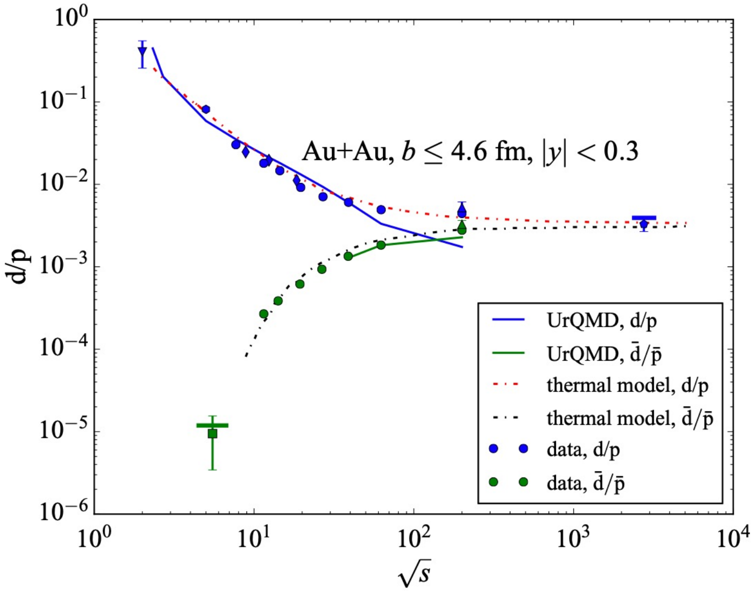

Anti-proton and anti-deuteron rapidity distribution for Si+Au reactions at E_{lab}=14.6 AGeV

d/p and anti-d/anti-p ratios as function of energy,

UrQMD vs data vs thermal model

- Substantial amount of anti-deuteron production even near threshold
- Relevance for dark matter...

S. Sombun, M. Bleicher et al, Phys. Rev. C 99 (2019) 014901

How well is the energy deposition described?

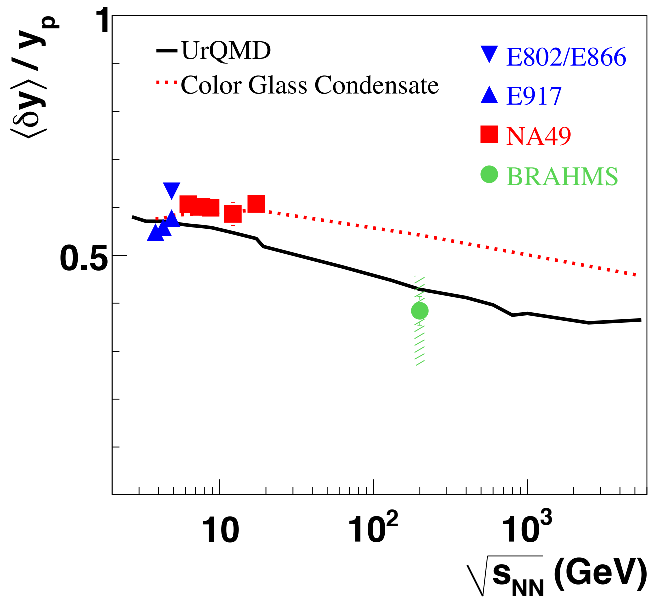

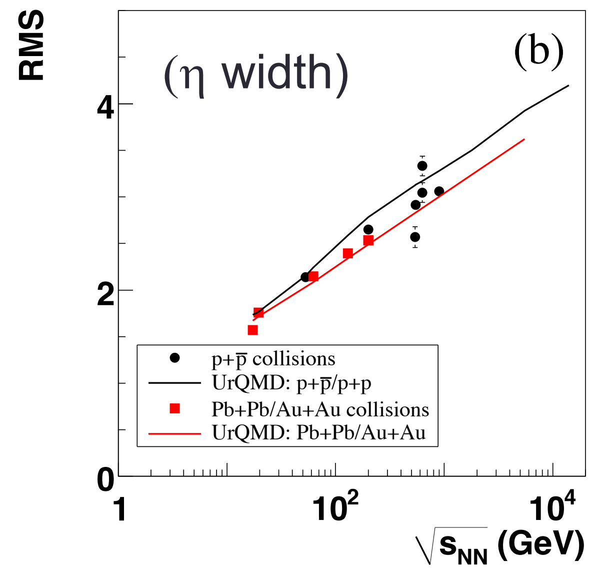

Rapidity shift of the baryons:

$$\langle \delta y \rangle = y_p - \frac{2}{\langle N_{\rm part} \rangle} \int_0^\infty y \frac{dN_{B-\bar{B}}}{dy} dy,$$

Width (root-mean-square) of the charged particle rapidity distributions for p+p and Au+Au reactions

- Good description of the energy loss of leading baryons
- consistency with growing width of charged particle rapidity density

M. Mitrovki, M. Bleicher et al, Phys.Rev. C79 (2009) 044901

Comparison to low/mid energy data (large systems)

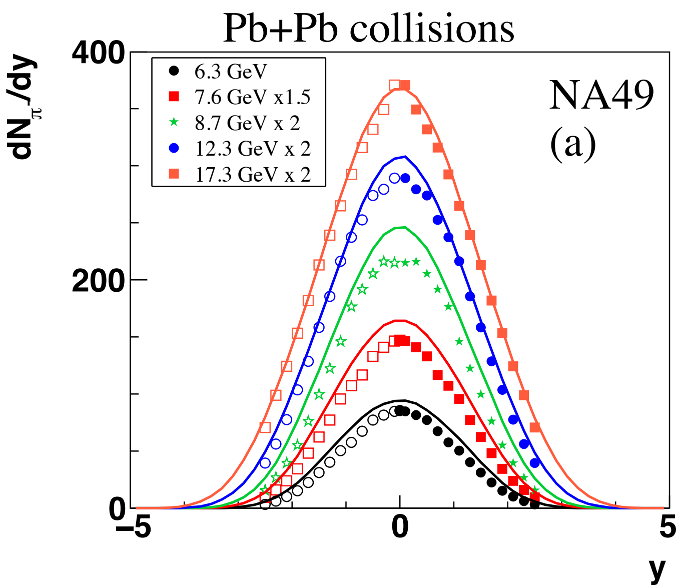

Charged pion rapidity distribution: Model vs. data from NA49 for different center-of-mass energies

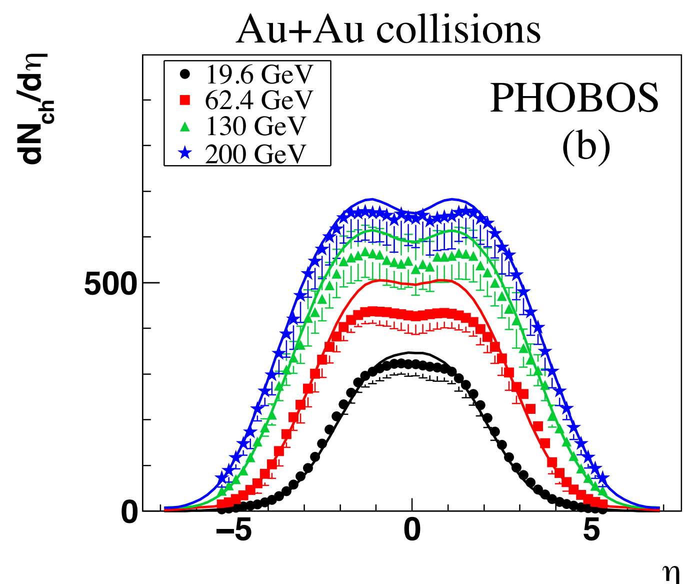

Charged particle pseudo-rapidity distribution: Model vs. data from PHOBOS for different center-of-mass energies

- Charged particle production at central and forward rapidities in line with data

M. Mitrovki, M. Bleicher et al, Phys.Rev. C79 (2009) 044901

Detailed multiplicity studies – low/mid energy

Left: Energy dependence of midrapidity particle yields in Au+Au/Pb+Pb reaction

Right: Energy dependence of integrated particle yields in Au+Au/Pb+Pb reaction

- Yields of different particle species are well reproduced, both at midrapidity and integrated over 4π

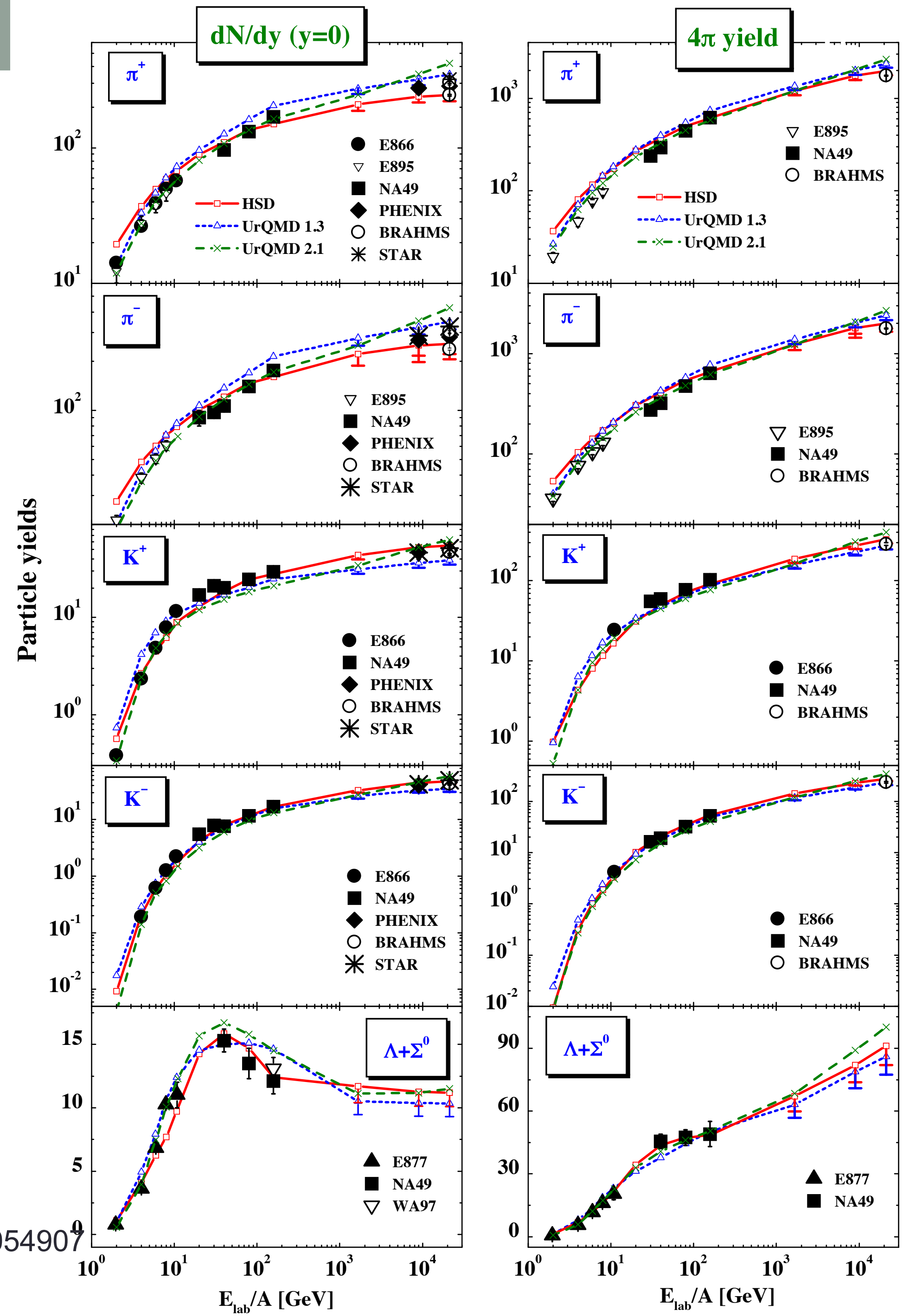

E. Bratkovskaya, M. Bleicher et al, Phys.Rev. C69 (2004) 054907

Detailed transverse momentum studies – low energy

- Energy dependence (from top to bottom) of transverse momentum spectra
  in Au+Au/Pb+Pb reactions

- Transverse momentum distributions of different particle species are well reproduced as compared to data.

E. Bratkovskaya, M. Bleicher et al, PRC69 (2004) 054907

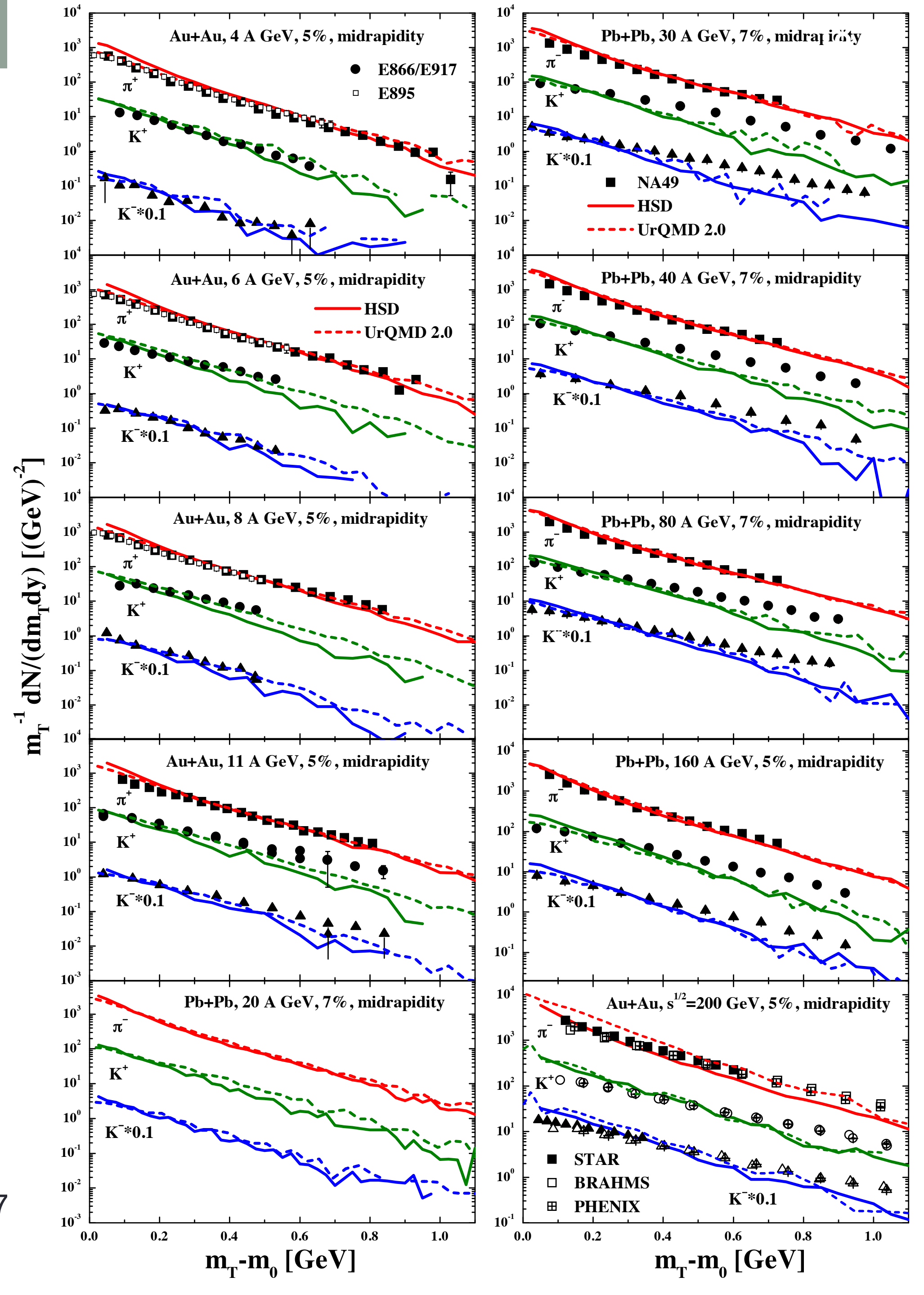

Small systems at high energies

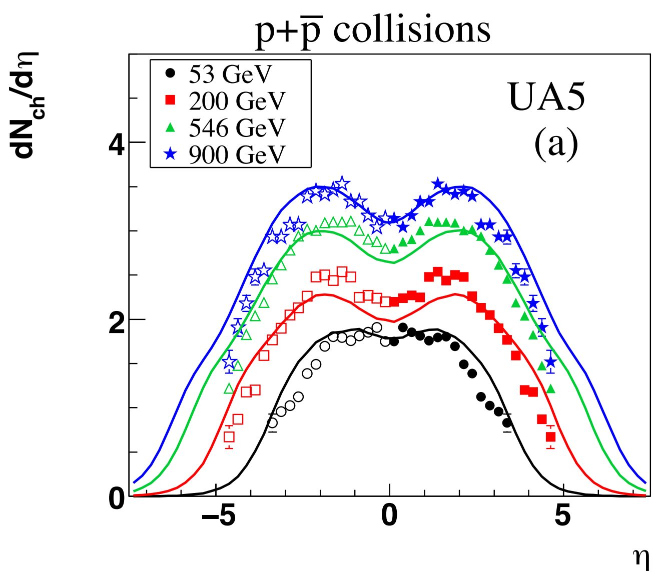

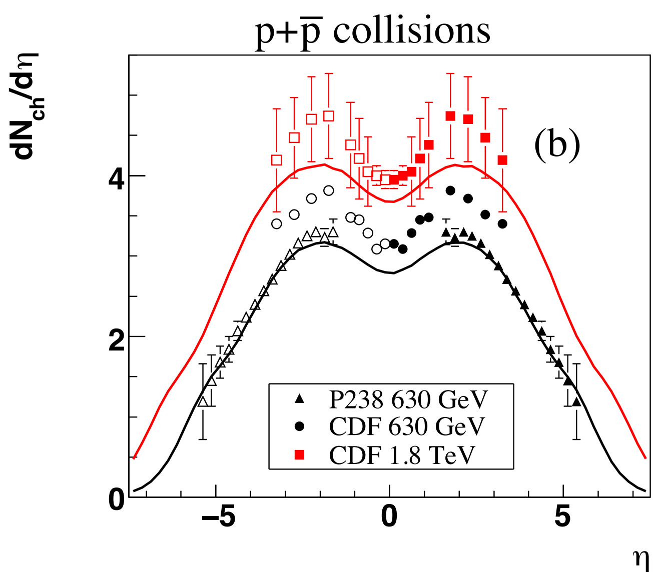

Pseudo-rapidity distribution of charged particles in anti-proton+proton collision

Pseudo-rapidity distribution of charged particles in anti-proton+proton collision

- Good description of charged particle rapidity distribution for small systems

M. Mitrovki, M. Bleicher et al, Phys.Rev. C79 (2009) 044901

Ultra-relativistic Quantum Molecular Dynamics (UrQMD) – hybrid mode

Hybrid mode calculations (RHIC and LHC energies)

- At energies above 50 GeV (CM-energy) the early intermediate state can not be modeled by strings and particles alone
- To take the local equilibration and the phase transition to a QGP into account, a hydrodynamic phase is introduced
- This is known as hybrid model (Transport+hydro), hybrid models have become the standard at RHIC and LHC energies

Petersen, Bleicher, et al, Phys.Rev. C78 (2008) 044901

UrQMD hybrid model

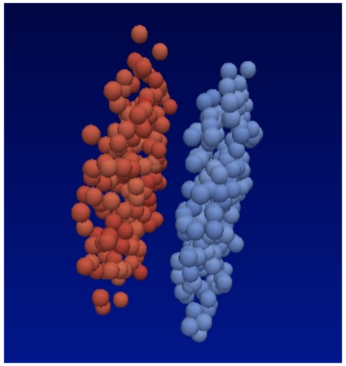

- Initial State:
  - Initialization of two nuclei
  - Non-equilibrium hadron-string dynamics
  - Initial state fluctuations are included naturally

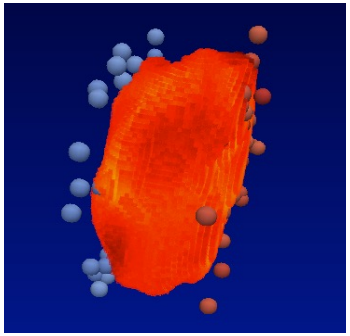

- 3+1d Hydro +EoS:
  - **SHASTA** ideal relativistic fluid dynamics
  - Net baryon density is explicitly propagated
  - Equation of state at finit μ_B

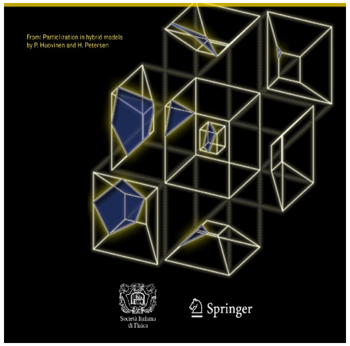

- Final State:
  - Hypersurface at constant energy density
  - Hadronic rescattering and resonance decays within UrQMD

H.Petersen, et al, PRC78 (2008) 044901
P. Huovinen, H. P. EPJ A48 (2012) 171

Hybrid model details: Initial State

- Contracted nuclei have passed through each other

$$t_{start} = \frac{2R}{\gamma v}$$

  - Energy is deposited
  - Baryon currents have separated
- Energy-, momentum- and baryon number densities are mapped onto the hydro grid
- **Event-by-event fluctuations** are taken into account
- Spectators are propagated separately in the cascade

(J.Steinheimer et al., PRC 77,034901,2008)

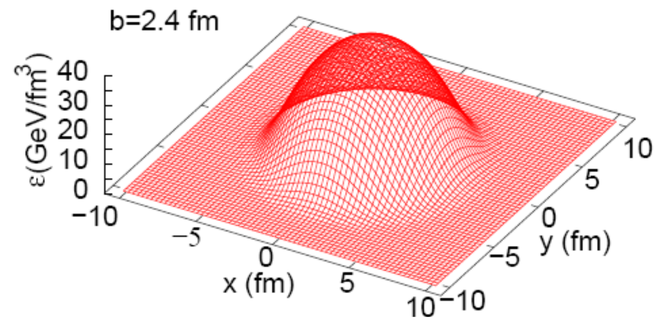

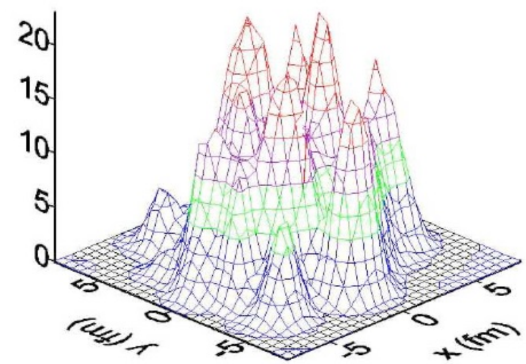

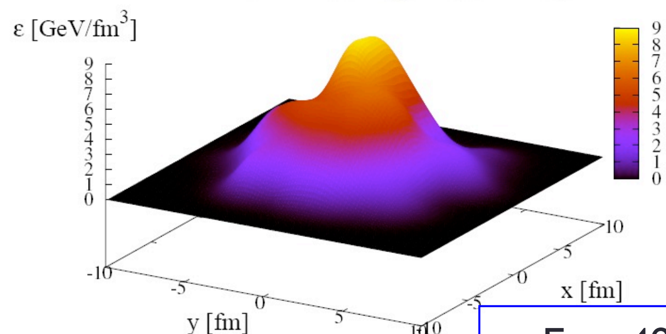

E_{lab}=40 AGeV
b=0 fm

(nucl-th/0607018, nucl-th/0511021)

Hybrid model details: Equations of State

Ideal relativistic one fluid dynamics:

$$\partial_\mu T^{\mu\nu} = 0 \quad \text{and} \quad \partial_\mu (n u^\mu) = 0$$

- HG: **Hadron gas** including the same degrees of freedom as in UrQMD (all hadrons with masses up to 2.2 GeV)
- CH: **Chiral EoS** from quark-meson model with first order transition and critical endpoint (most realistic)
- BM: **Bag Model EoS** with a strong first order phase transition between QGP and hadronic phase

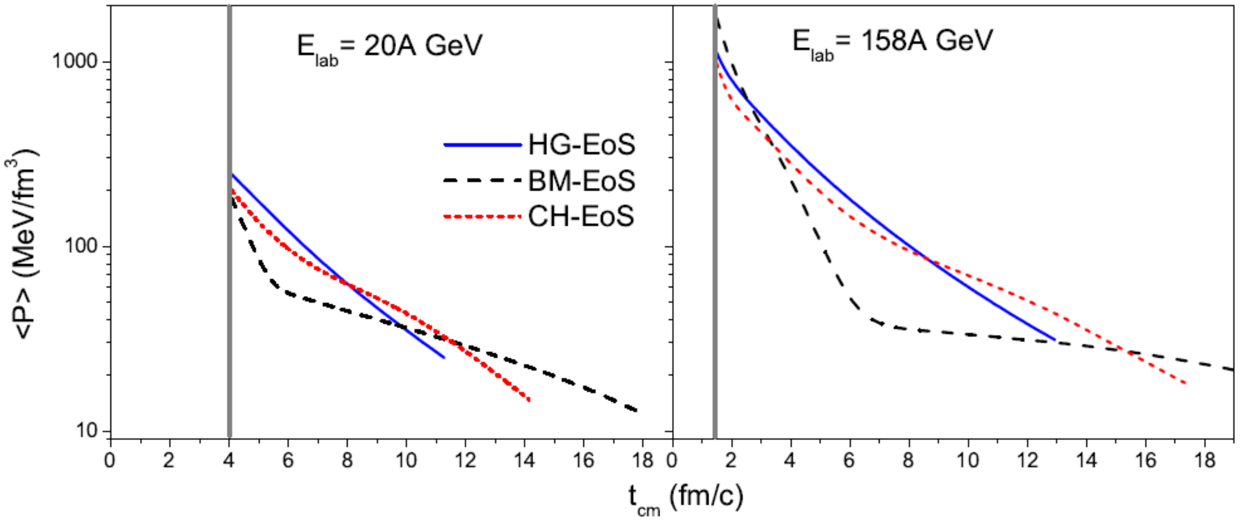

D. Rischke et al., NPA 595, 346, 1995,

D. Zschiesche et al., PLB 547, 7, 2002

Papazoglou et al., PRC 59, 411, 1999

J. Steinheimer, et al., J. Phys. G38 (2011) 035001

Hadronization and Cooper-Frye

Experiments observe **finite number** of hadrons in detectors

Hadronization controlled by the equation of state

Sampling of particles according to **Cooper-Frye** should:

-Respect **conservation laws**,
maybe even locally?

-Introduces fluctuations on its own

$$E\frac{dN}{d^3p} = \int_\sigma f(x,p)p^\mu d\sigma_\mu$$

Cooper-Frye hyper-surface at transition from hydro to transport

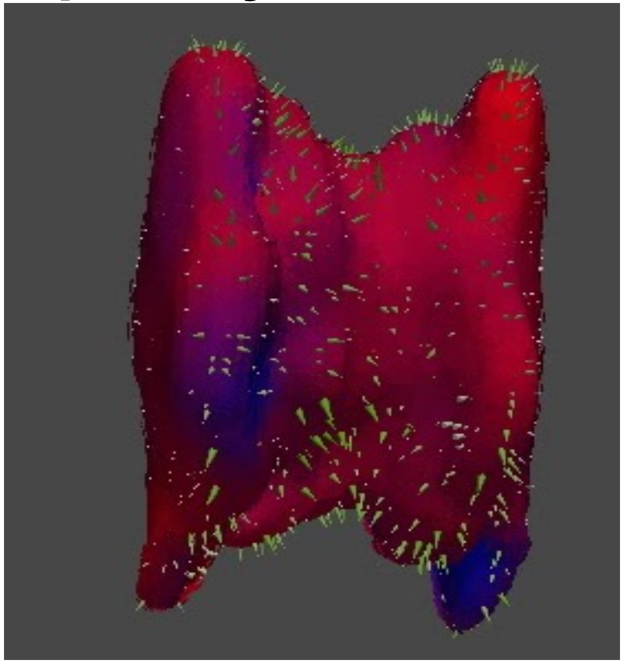

Sophisticated 3D hypersurface finder to resolve interesting structures in event-by-event simulations
Petersen, Huovinen, arXiv:1206.3371

Time evolution UrQMD hybrid model

Nuclei at 99 % speed of light

Quark Gluon Plasma

Hadronic Rescattering

Measurable Fragments in the detector

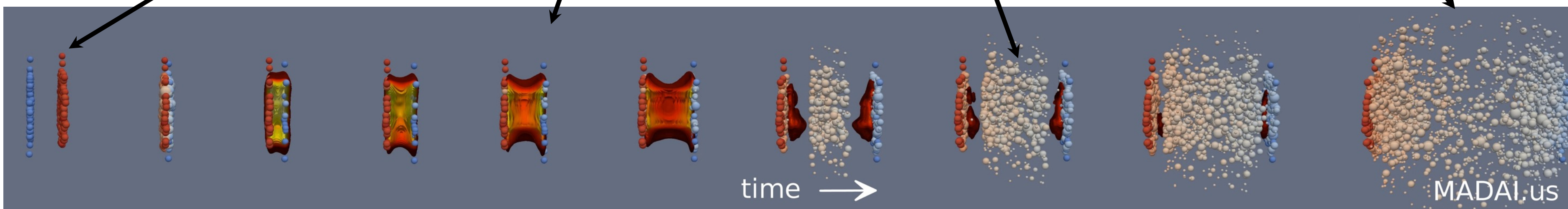

1x 10^{-23} s

10 x 10^{-23} s

30 x 10^{-23} s

Nonequilibrium initial state dynamics → Relativistic Hydrodynamics → Hadron Transport

Hybrid approaches are very successful for the description of the dynamics

H. Petersen, special issue JPG, arXiv:1404.1763

Summary

- UrQMD is a well benchmarked model for the description of hadron-hadron, hadron-nucleus and nucleus-nucleus collisions.
- Particle yields, spectra and baryon-stopping in line with data (especially at low/mid energies)
- In hybrid mode it is applicable up to LHC energies
- In standard cascade mode (no hydro) the model needs seconds for the simulation of a single event.
- However, hybrid calculations are slow at LHC energies (up to 1h per event)

→Tuning: Difficult